LATERAL CONTROL OF AN AUTONOMOUS VEHICLE USING INTEGRATED BACKSTEPPING AND SLIDING MODE CONTROLLER

Armin Norouzi[1*], Milad Masoumi[2], Ali Barari[3], and Saina Farrokhpour Sani[4]

[1] Department of Mechanical Engineering, Faculty of Engineering, University of Alberta, Edmonton, Canada
[2] Department of Electrical Engineering, Azad University of Garmsar, Garmsar, Iran
[3] Department of Mechanical Engineering, K. N. Toosi University of Technology, Tehran, Iran
[4] School of Railway Engineering (SRE), Iran University of Science & Technology, Tehran, Iran
*** Corresponding author:** Armin Norouzi, Mechanical Engineering Building, North Campus,University of Alberta, Edmonton, AB T6G 2G8, Canada. Email: norouziy@ualberta.ca

ABSTRACT - In this paper, a novel Lyapunov-based robust controller by using meta-heuristic optimization algorithm has been proposed for lateral control of an autonomous vehicle. In the first step, double lane change path has been designed using a 5th-degree polynomial (quantic) function and dynamic constraints. A lane changing path planning method has been used to design the double lane change manoeuvre. In the next step, position and orientation errors have been extracted based on the 2-DOF vehicle bicycle model. A combination of sliding mode and backstepping controllers has been used to control the steering in this paper. Overall stability of the combined controller has been analytically proved by defining a Lyapunov function and based on Lyapunov stability theorem. The proposed controller includes some constant parameters which have effects on controller performance; therefore, particle swarm optimization (PSO) algorithm has been used for finding optimum values of these parameters. The comparing result of the proposed controller with backstepping controller illustrated the better performance of the proposed controller, especially in the low road frictions. Simulation of designed controllers has been conducted by linking CarSim software with Matlab / Simulink which provides a nonlinear full vehicle model. The simulation was performed for manoeuvres with different durations and road frictions. The proposed controller has outperformed the backstepping controller, especially in low frictions.

KEYWORDS: Vehicle lateral control, Autonomous vehicle, Backstepping controller, Sliding mode controller, Lyapunov based controllers.

1. INTRODUCTION

There are many contributing factors to grounded vehicle accidents including poor road condition and violation of necessary rules such as speeding and especially unsafe lane change. Driver error was cited as the underlying cause of from 45% to 75% of fatal crashes [1]. To reduce driver-related accidents, numerous researches have been conducted to deal with this problem. Advanced driver assistance systems (ADASs) have been proposed by transportation experts to address this issue. ADASs can provide autonomous control due to three methods[2]. Firstly, the autonomous vehicle controller obtains surrounding information. Next, the controller design desired path based on environmental information. Finally, the controller needs to track the desired path. In this paper, just the controller's ability to track the desired path has been studied.

Vehicle dynamics is one of the primary and fundamental parts of classical mechanics which argues about the dynamics of vehicles. Controllers play a crucial role in the responding system and have a significant impact on the input and output of the control systems. In Vehicle Dynamic Control, lateral control of the vehicle is an essential part, because of its role in the stability of the vehicle. In vehicle dynamics control, the yaw stability control system is an essential part of vehicle stability. Lateral dynamic control of vehicles is generally done through braking and steering subsystems. In yaw control system strategies, the controller needs to control yaw rate and sideslip angle quickly and responsively to follow the designed path by using steering and braking systems [3]. Controlling steering has significant impacts on control of the vehicle on the designed path direction, and it is the main discussion of the current paper.

Advanced active chassis control systems include 4WS[1], AFS[2], SBW[3] and DYC[4] in which steering

[1] four wheel steering
[2] active front steering
[3] steer-by-wire
[4] direct yaw moment control

system plays the central role. Generally, there are three structures in the active steering systems that include 4WS, ARS[5] and 4WAS[6] [4]. Vehicle active steering plays a crucial role in accident avoidance, vehicle handling, and vehicle stability when facing changes in road conditions or the presence of an obstacle [5]. Vehicle active steering has applications in tracking the manoeuvres, especially in autonomous vehicles, and is very useful in tracking the optimum path. The most common chassis control is four-wheel steering (4WS) the 4WS depends on tire lateral force which is proportional to the steer angle in a range where the lateral acceleration is small. Under this circumstance, the control law can be introduced rather easily by adopting a 2 DOF linear vehicle model[6] Lyapunov method is a very useful tool for feedback controller design. Many of the feedback control techniques are based on the idea of a Lyapunov function definition or, more specifically, are based on the derivative of the Lyapunov function which guarantees the convergence to an equilibrium point or a point of stability. Backstepping and sliding mode controllers are feedback controllers based on the Lyapunov. The backstepping controller is designed based on the Lyapunov function definition. The backstepping controller can use high flexibility to solve stability, tracking and robust control with lower limitations than other methods. Sliding mode controller is a prevalent method in robust control design. Sliding mode control, the sliding surface gets to an equilibrium point in a limited time and keeps the system in future time on that point [7].

Robust control methods in the design of the lateral Vehicle controller, particularly control methods based on Lyapunov stability are beneficial due to the presence of uncertainties in vehicle systems. Guo et al. [8] used an integrated longitudinal, and lateral movements designed a path tracking system based on the integral backstepping controller. Another study designed and tested a backstepping controller for lane change manoeuvre and their results of tests presented the proper convergence of errors [9]. Unlike backstepping controllers, sliding mode controllers and their integration with other control laws have been extensively used by researchers. Using sliding mode control based on Lyapunov stability, proper results of stability and path tracking are presented in [10-14]. However, its integration with the adaptive control law [15], fuzzy systems [16], adaptive fuzzy systems [17], the PI controller [18] and fuzzy neural networks [19] improved the results compared to the classical sliding mode controller. In [15] switching gain is updated based on the sliding surface. This controller does not need an upper limit of uncertainty in determining switching gain as well as the adaptive sliding surface has a good performance. Based on the designed controller by Li and et al. [16], sliding surface and its derivations enter a fuzzy logic system and its output execute the command to do the manoeuvre. In Fuzzy neural networks sliding mode controller, sliding surface enters a fuzzy neural network controller, and its output generates the vehicle command. Results indicated better performance compare to the sliding mode controller [19]. In the adaptive fuzzy sliding mode controller [17], system error enters the fuzzy controller after creating sliding surface, and fuzzy controller factors are updated based on the system error. Finally, adding this controller to the equivalent sliding mode controller provides vehicle commands. Alipour et al. [18], used a combination of PI controller and sliding mode controller to create an improved sliding mode controller which showed more precise results compared to the sliding mode controller. Meta-heuristic optimization algorithms are used enormously to design controllers [20, 21]. Feng and et al. Genetic Algorithm has been used to optimize the fuzzy-neural network (FNN) controller for tracking the vehicle's manoeuvre in lane changing [20]. PID and LQR controllers are optimized using PSO algorithm [21]. Of course, one of the fundamental problems in the use of optimization algorithms is that they take much time to respond and convergence which makes them unusable in real-time systems.

In this study, the backstepping controller is combined with a sliding mode controller to design a lateral controller for tracking the reference path. The PSO algorithm is used to optimize control system parameters. The cost function of this optimization is the sliding surfaces of the sliding mode controller and the controller output. Based on the references, both backstepping and sliding model controller has good control performance in controlling nonlinear systems. Therefore, combining these two controllers and using a meta-heuristic optimization algorithm for finding the constant coefficient have achieved the perfect tracking of desired inputs. On the other hand, analytical proof of lyapunov stability for integration controller guarantee the stability of the proposed controller. In this study, the two-degree vehicle model and lateral position and orientation error model with constant longitudinal velocity have been used. Controller simulation has been conducted using a full vehicle model by linkage of Matlab/Simulink with CarSim. The desired path is a double lane change manoeuvre which is used for overtaking manoeuvres. Simulation results indicated accurate tracking compare to the backstepping controller in low (0.3) and high (0.9) frictions and also in different manoeuvre durations.

.

[5] active rear steering

[6] active front steering and four- wheel active steering

2. PATH PLANNING

There are specified standard lane change manoeuvres regarding geometry and kinematics as stated in ISO and BS standards, used with full non-linear multi-body models which are more representative of real vehicle dynamics[22] but in this study, a five-degree polynomial function (Quintic) is used for lane change maneuvers[23]. Eq. (1) is considered for lane changing path planning. At the start and finish time vehicle moves in a straight line so lateral acceleration and speed will be equal to zero. Lateral position is equal to zero at the beginning (Eq. 2), and the spacing between two lanes is considered for at the end for it (Eq. 3). t_i is the start time, and t_f is the end time of the manoeuvre.

$$y(t) = at^5 + bt^4 + ct^3 + dt^2 + et + f \tag{1}$$

$$\begin{aligned} \dot{y}|_{t=t_i} &= 0 \\ \ddot{y}|_{t=t_i} &= 0 \\ \dot{y}|_{t=t_f} &= 0 \\ \ddot{y}|_{t=t_f} &= 0 \end{aligned} \tag{2}$$

$$\begin{aligned} y|_{t=t_i} &= w_1 \\ y_1|_{t=t_f} &= w_2 \end{aligned} \tag{3}$$

w_1 and w_2 are equal to zero and 3.75 for the manoeuvre and for the second lane change manoeuvre they are equal to 3.75 and zero. By applying the boundary conditions to the candidate Eq. (1), the final manoeuvre path is obtained. In this study, manoeuvres of three seconds duration (t_f-t_i = 3) and five seconds duration (t_f-t_i = 5) are considered for both direct and reverse path. Manoeuvres are shown in Figure 1.

3. MODELING

3.1. Vehicle's model for designing controller

The state-space of vehicle 2-DOF bicycle model has been adopted for designing controller [24]. Nevertheless, in real-time, a bicycle model is used where lateral accelerations are relatively low[25]. Schematic of this model is shown in Figure 2.

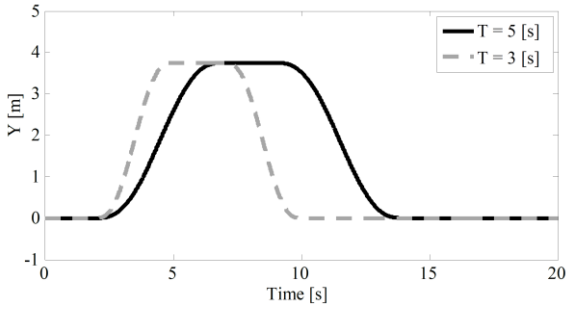

Figure 1. Double lane change designed reference path

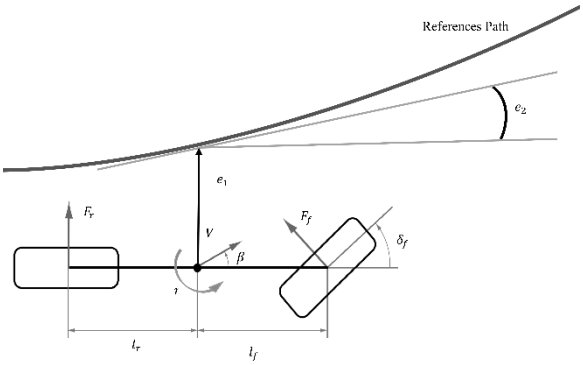

Figure 2. A schematic view of a 2-DOF vehicle bicycle model and lateral position and orientation errors

$$\frac{d}{dt}\begin{Bmatrix} y \\ \dot{y} \\ \psi \\ \dot{\psi} \end{Bmatrix} = \begin{Bmatrix} 0 \\ \frac{2C_f}{m} \\ 0 \\ \frac{2l_f C_f}{I_z} \end{Bmatrix} \delta + \begin{bmatrix} 0 & 1 & 0 & 0 \\ 0 & -\frac{2C_f + 2C_r}{mV_x} & 0 & -V_x - \frac{2l_f C_f - 2C_r l_r}{mV_x} \\ 0 & 0 & 0 & 1 \\ 0 & -\frac{2l_f C_f - 2l_r C_r}{I_z V_x} & 0 & -\frac{2l_f^2 C_f + 2l_r^2 C_r}{I_z V_x} \end{bmatrix} \tag{4}$$

For controlling the vehicle to follow the path, orientation and positioning errors are defined based on the distance of the mass centre from the desired path and the angle of the desired path from the vehicle angle in Eq. (5) [24].

$$\ddot{e}_1 = \ddot{y} + V_x(\dot{\psi} - \dot{\psi}_d) \ , \ e_2 = \dot{\psi} - \psi_d \tag{5}$$

Vehicle error model is obtained by writing vehicle models based on the Eq. (5):

$$\frac{d}{dt}\begin{Bmatrix} e_1 \\ \dot{e}_1 \\ e_2 \\ \dot{e}_2 \end{Bmatrix} = \begin{Bmatrix} 0 \\ \frac{2C_f}{m} \\ 0 \\ \frac{2l_f C_f}{I_z} \end{Bmatrix} \delta + \begin{bmatrix} 0 \\ -\frac{2C_f l_f - 2C_r l_r}{mV_x} - V_x \\ 0 \\ -\frac{2C_f l_f^2 + 2C_r l_r^2}{V_x I_z} \end{bmatrix} \dot{\psi}_d + \begin{bmatrix} 0 & 1 & 0 & 0 \\ 0 & -\frac{2C_f + 2C_r}{mV_x} & \frac{2C_f + 2C_r}{m} & \frac{-2C_f l_f + 2C_r l_r}{mV_x} \\ 0 & 0 & 0 & 1 \\ 0 & -\frac{2C_f l_f - 2C_r l_r}{I_z V_x} & \frac{2C_f l_f - 2C_r l_r}{I_z} & -\frac{2C_f l_f^2 + 2C_r l_r^2}{I_z} \end{bmatrix} \begin{bmatrix} e_1 \\ \dot{e}_1 \\ e_2 \\ \dot{e}_2 \end{bmatrix} \tag{6}$$

3.2. Tyre model

2-DOF bicycle model has been used for designing controller. This model has proposed based on linear tyre model[24]. The controller has been applied to carsim by linking CarSim software with Matlab / Simulink. Therefore, the controller has been tested based on nonlinear tyre mode. The CarSim has been developed based on several tyre models. The extended model (more tables for camber effects), the Pacejka 5.2 version of the magic formula, and MF-Tyre from TASS/TNO has been used in running.

4. CONTROLLER DESIGN

4.1. Preparing the model for controller design

For backstepping controller design, the control system should be considered as follows [7]:

$$\dot{\eta} = f(\eta) + G(\eta)\xi \tag{7}$$

$$\dot{\xi} = f_a(\eta,\xi) + G_a(\eta,\xi)\, u \tag{8}$$

For designing the backstepping controller, the Eq. 6 should be written as Eqs. (7) and, (8), therefore

$$\dot{x}_1 = \begin{bmatrix}1 & 0 & 0\end{bmatrix}\begin{bmatrix}x_2\\ x_3\\ x_4\end{bmatrix} \tag{9}$$

$$\begin{bmatrix}\dot{x}_2\\ \dot{x}_3\\ \dot{x}_4\end{bmatrix} = \begin{bmatrix}a_{11} & a_{12} & a_{13}\\ 0 & 0 & 1\\ a_{21} & a_{22} & a_{23}\end{bmatrix}\begin{bmatrix}x_2\\ x_3\\ x_4\end{bmatrix} + \begin{bmatrix}b_1\\ 0\\ b_2\end{bmatrix} u + \begin{bmatrix}d_1\\ 0\\ d_2\end{bmatrix}\dot{\psi}_d \tag{10}$$

X matrix is defined as follows:

$$\vec{X} = \begin{bmatrix}x_1\\ x_2\\ x_3\\ x_4\end{bmatrix} = \begin{bmatrix}e_1\\ \dot{e}_1\\ e_2\\ \dot{e}_2\end{bmatrix} \tag{11}$$

The correlation coefficients of Eq. (10) is presented in Table 1.

By comparing Eq. (9) and (10) with Eq. (7) and 8, the following equations are obtained:

$$\eta = x_1, f(\eta) = 0, G(\eta) = \begin{bmatrix}0 & 1 & 0\end{bmatrix}$$

$$f_a = \begin{bmatrix}a_{11} & a_{12} & a_{13}\\ 0 & 0 & 1\\ a_{21} & a_{22} & a_{23}\end{bmatrix}\begin{bmatrix}x_2\\ x_3\\ x_4\end{bmatrix} \tag{12}$$

$$G_a(\eta,\xi) = \begin{bmatrix}b_1\\ 0\\ b_2\end{bmatrix}, \xi = \begin{bmatrix}x_2\\ x_3\\ x_4\end{bmatrix}$$

Table 1. Nomenclature of the vehicle's dynamic model

	equation		equation
a_{11}	$-2\mu\frac{C_{\alpha f}+C_{\alpha r}}{mV_x}$	a_{21}	$2\mu\frac{l_rC_{\alpha r}-l_fC_{\alpha f}}{I_zV_x}$
a_{12}	$2\mu\frac{C_{\alpha f}+C_{\alpha r}}{m}$	a_{22}	$2\mu\frac{l_fC_{\alpha f}-l_rC_{\alpha r}}{I_z}$
a_{13}	$2\mu\frac{l_rC_{\alpha r}-l_fC_{\alpha f}}{mV_x}$	a_{23}	$-2\mu\frac{C_{\alpha f}l_f^2+C_{\alpha r}l_r^2}{I_zV_x}$
b_1	$2\mu\frac{c_f}{m}$	b_2	$2\mu\frac{l_fc_f}{I_z}$
d_1	$2\mu\frac{l_rC_{\alpha r}-l_fC_{\alpha f}}{mV_x}-V_x$	d_2	$-2\mu\frac{C_{\alpha f}l_f^2+C_{\alpha r}l_r^2}{I_zV_x}$

Two systems of two-degree-of-freedom bicycle model equations are converted to backstepping controller standardly based on the [7].

4.2. Design of Backstepping Controller

The controllers that resist against disturbances and uncertainty of parameters are called robust controllers. The backstepping controller is a robust controller. Eq. (7) and (8) are considered as the standard equations of the system in which $\eta \in R^n$, $\zeta \in R^m$ and $u \in R^m$ (m can be greater than 1). Suppose that f, f_a, G, G_a are smooth functions (and defined) on the domain of the question, and also f and f_a are zero at the origin and matrix $G_a(m\times m)$ is non-singular. Also, suppose that the system equation (Eq. 8) can stabilize using a feedback controller $\zeta = \phi(\eta)$ by $\phi(0) = 0$ while Lyapunov function (smooth and positive defined) $V(\eta)$ is applied in the following inequality:

$$\frac{\partial V}{\partial \eta} = \left[f(\eta) + G(\eta)\phi(\eta)\right] \le -W(\eta) \tag{13}$$

The Lyapunov candidate function is defined based on systems equation (Eq. (7) and (8)) as follow [7]:

$$V_a = V(\eta) + \frac{1}{2}\left[\eta - \varphi(\eta)\right]^T\left[\xi - \varphi(\eta)\right] \tag{14}$$

By differentiating the Lyapunov candidate function, the desired input is obtained which satisfy the stability theorem of Lyapunov condition:

$$\dot{V}_a = \frac{\partial V}{\partial \eta} = (f + G\phi) + \frac{\partial V}{\partial \eta} C(\xi - \phi) + [\xi - \phi]^T \left[f_a + G_a u - \frac{\partial \phi}{\partial \eta}(f + G\xi) \right] \quad (15)$$

Considering Eq. (15), the control law is obtained as:

$$u = G_a^{-1} \left[\frac{\partial \phi}{\partial \eta}(f + G\xi) - (\frac{\partial V}{\partial \eta} G)^T - f - k(\xi - \phi) \right] \quad (16)$$

$$k > 0$$

Applying the above control law, the stability of the system is proved using the Lyapunov stability theorem.

$$\dot{V}_a = \frac{\partial V}{\partial \eta}(f + G\phi) - k(\xi - \phi)^T(\xi - \varphi) \le W(\eta) - k(\xi - \phi)^T(\xi - \phi) \quad (17)$$

Eq. 17 indicates that the origin ($\xi = 0, \eta = 0$) has asymptotic stability.

Using the system obtained in Eq. (9) and Eq. (10), and employing Eq. (11) the backstepping controller could be applied to 2 DOF model of vehicle. The feedback control law stabilizer and the Lyapunov function $V(\eta)$ is defined as:

$$\xi = \phi = -\begin{bmatrix} x_1 \\ x_1 \\ x_1 \end{bmatrix} \quad (18)$$

$$V(\eta) = \frac{1}{2}\phi^T\phi = \frac{3}{2}x_1^2 \quad (19)$$

Applying Eq. (18) to Eq. (9) yields:

$$\dot{x}_1 = G(\eta)\phi = -x_1 \quad (20)$$

To prove the Lyapunov stability, Eq. (19) is differentiated:

$$\dot{V}(\eta) = 3x_1\dot{x}_1 \quad (21)$$

Using Eq. (20) and (21), the Lyapunov stability is proved:

$$\dot{V}(\eta) = 3x_1^2 \le 0 \quad (22)$$

Now, considering the system of Eq. (9) and (10), and Eq. (16) and (18), the control input is obtained as:

$$u_B = G_a^T \left\{ \left(\begin{bmatrix} 0 & 1 & 0 \end{bmatrix} \begin{bmatrix} x_2 \\ x_3 \\ x_4 \end{bmatrix} \right) \begin{bmatrix} -1 \\ -1 \\ -1 \end{bmatrix} - \begin{bmatrix} 0 \\ 1 \\ 0 \end{bmatrix} (-3x_1) \right\} - \begin{bmatrix} a_{11} & a_{12} & a_{13} \\ 0 & 0 & 1 \\ a_{21} & a_{22} & a_{23} \end{bmatrix} \begin{bmatrix} x_2 \\ x_3 \\ x_4 \end{bmatrix} - k \begin{bmatrix} x_2 + x_1 \\ x_3 + x_1 \\ x_4 + x_1 \end{bmatrix} \quad (23)$$

Simplifying Eq. (23), the control law of backstepping controller is obtained:

$$\hat{u}_B = \left(-k(b_1 + b_2)\right)e_1 - (b_1 + b_2 + b_1a_{12} + b_2a_{22})\, e_2 - \left(b_1a_{11} + b_2a_{21} + b_1k\right)\dot{e}_1 - (b_1a_{13} + b_2a_{23} + b_2k)\, \dot{e}_2 \quad (24)$$

$$u_B = \frac{\hat{u}_B}{(b_1^2 + b_2^2)} \quad (25)$$

Where u_B is the control input yielded from backstepping controller. The value of k is considered so large that can be robust against uncertainties.

4.3. Designing the backstepping controller integrated with sliding mode controller

Similar to the backstepping controller, based on stabilizing of $\zeta = \phi(\eta)$ provided that $\phi(0) = 0$. We are also pursuing the function $V(\eta)$, such that for any $v(\eta,\xi) \in D$ and constant c thus:

$$\dot{V} \le c\|\eta\|_2^2 \quad (26)$$

The above equation indicates that η=0 is the asymptotic stable equilibrium point of the following system:

$$\dot{\eta} = f(\eta) + G(\eta)\, \phi(\eta) \quad (27)$$

The sliding surface is defined as Eq. (28), which is, in fact, the difference between ξ and $\varphi(\eta)$.

$$S = \xi - \varphi(\eta) \quad (28)$$

In addition, the Lyapunov candidate function is considered as Eq. (29):

$$V_a(\eta, \xi) = V(\eta) + \frac{1}{2}(S)^2 \quad (29)$$

So, the derivatives of V_a in direction of Eq. (7) and (8) is obtained as

$$\dot{V}_a = \dot{V} + (\xi - \varphi)\left[f_a + G_a u - \frac{\partial \varphi}{\partial \eta}(f + G\xi) \right] \quad (30)$$

and the control input is as

$$u = G_a^{-1} \left[\frac{\partial \phi}{\partial \eta}(f + G\xi) - \frac{\partial V}{\partial \eta} G - f_a - k\, \mathrm{sgn}(\xi - \varphi) \right] \quad (31)$$

$$k \ge 0$$

Using Eq. (26) and (31), the designed controller's stability (Eq. 30) can be proved using the Lyapunov stability theorem as:

$$\begin{aligned} V_a = \dot{V} + S\dot{S} &\le -c\|\eta\|_2^2 + S(\dot{\xi} - \dot{\eta}\frac{\partial \varphi}{\partial \eta}) \\ &\le -c\|\eta\|_2^2 + S(f_a + G_a u - (f - G\xi) - \frac{\partial \varphi}{\partial \eta}) \\ &\le -c\|\eta\|_2^2 + s(-k\, \mathrm{sgn}(S)) \\ &\le -c\|\eta\|_2^2 + (-k)\, |S| \end{aligned} \quad (32)$$

Choosing $k \ge 0$ thus:

$$\dot{V}_a \le -\sigma\left[\|\eta\|_2^2 + |S| \right] \quad (33)$$

Where σ is positive. So, according to Lyapunov stability theorem, this system is always stable. In the presence of disturbances, the condition k for the stability of both controllers (i.e. backstepping controller and backstepping controller integrated with sliding mode controller) must be greater than upper bounds of the disturbance. Choosing a greater k, one would resist against disturbances, but the control input

would have also high value. In this paper, making advantages of defining an appropriate cost function and applying the Particle Swarm Optimization (PSO) meta-heuristic method. PSO is an iterative computing method which optimizes a problem through improving possible solutions in terms of certain quality criteria. Considering an initial population of possible solutions as particles and moving them in search space, the PSO method optimizes and solves the problem using a simple formula in terms of the position and velocity of each particle. The movements of particles are influenced by the local and global best position known so far. These positions are updated each time a new position is found. Therefore, one expects for the particles to move towards the best possible solution.

In order to prove that the slip surface is converged towards zero, the Lyapunov function is considered as follows. Through differentiating the equations, the stability is proved analytically.

$$\begin{aligned} V_s &= \frac{1}{2}S^2 \\ &= S\dot{S} = S(\dot{\xi} - \dot{\eta}\frac{\partial \varphi}{\partial \eta}) \\ &= S(f_a + G_a u - (f + G\xi)\frac{\partial \varphi(\eta)}{\partial \eta}) \\ &\le S(-k\,\mathrm{sgn}(S)) \\ &\le -k|S| \end{aligned} \tag{34}$$

By choosing a k greater than zero, the sliding surface is converged towards zero.

In order to design the controller for the bicycle model of vehicle, the $\zeta = \phi(\eta)$ applied on the backstepping control (Eq. 18) is employed. Using Eq. (28), the sliding surface is obtained.

$$S = \begin{bmatrix} s_1 \\ s_2 \\ s_3 \end{bmatrix} = \xi - \varphi(\eta) = x_1 \begin{bmatrix} 1 \\ 1 \\ 1 \end{bmatrix} + \begin{bmatrix} x_2 \\ x_3 \\ x_4 \end{bmatrix} = \begin{bmatrix} x_2 + x_1 \\ x_3 + x_1 \\ x_4 + x_1 \end{bmatrix} \tag{35}$$

Considering the matrix G_a, the sliding surface s_2 is zero, because the second row of G_a matrix is zero. Thus, it has no effect on the control input. The input control of the integrated controller is obtained using Eq. (31).

$$u_{BS} = G_a^T \left[\begin{bmatrix} -1 \\ -1 \\ -1 \end{bmatrix} \left(\begin{bmatrix} 0 & 1 & 0 \end{bmatrix} \begin{bmatrix} x_2 \\ x_3 \\ x_4 \end{bmatrix} \right) - \left(\begin{bmatrix} 0 \\ 3x_1 \\ 0 \end{bmatrix} \right) - \begin{bmatrix} a_{11} & a_{12} & a_{13} \\ 0 & 0 & 1 \\ a_{21} & a_{22} & a_{23} \end{bmatrix} \begin{bmatrix} x_2 \\ x_3 \\ x_4 \end{bmatrix} - k \begin{bmatrix} \mathrm{sgn}(s_1) \\ \mathrm{sgn}(s_2) \\ \mathrm{sgn}(s_3) \end{bmatrix} \right] \tag{36}$$

Where u_{BS} is the control input of the proposed controller. Simplifying the Eq. (37), the control input is obtained as

$$\begin{aligned} \hat{u}_{B,S} &= -(b_1a_{12} + b_2a_{22} + b_1 + b_2)x_3 \\ &\quad -(b_1a_{13} + b_2a_{23})\,x_4 - (b_1a_{11} + b_2a_{21})x_2 \\ &\quad -k\left(b_1\,\mathrm{sgn}(x_2 + x_1) + b_2\,\mathrm{sgn}(x_4 + x_1)\right) \\ u_{B.S} &= \frac{\hat{u}_{B.S}}{(b_1^2 + b_2^2)} \end{aligned} \tag{37}$$

Taking into account the chattering phenomenon in the sliding mode controller, the Sat function has been used rather than the Sign function. Noting that the value of s_2 is equal to zero, the sliding surfaces are redefined as:

$$\begin{aligned} s_1 &= x_2 + x_1 \\ s_2 &= x_4 + x_1 \end{aligned} \tag{38}$$

$$\begin{aligned} u_{B.S} = &-\frac{(b_1a_{12} + b_2a_{22})}{b_1^2 + b_2^2}\dot{e}_1 - \frac{(b_1a_{13} + b_2a_{23})}{b_1^2 + b_2^2}\dot{e}_2 \\ &-\frac{(b_1a_{12} + b_2a_{22} + b_1 + b_2)}{b_1^2 + b_2^2}e_2 \\ &-\frac{k\left(b_1\,\mathrm{sat}(\frac{s_1}{\lambda}) + b_2\,\mathrm{sat}(\frac{s_2}{\lambda})\right)}{b_1^2 + b_2^2} \end{aligned} \tag{39}$$

where λ indicates the thickness of the boundary layer. The k value in Eq. (39) is obtained using the PSO method and the cost function shown in Eq. (40). The cost function is defined in terms of minimizing the sliding surface and control input.

$$\mathrm{Cost\,func.} = \int_0^t \left(|s_1| + |s_2| + |u|\right)dt \tag{40}$$

The controlling diagram of the proposed control law is shown in Figure 3.

5. SIMULATION AND RESULTS

In this paper, the Simulink and CarSim software have been linked together to simulate the system using the full vehicle model. The equations of motion in the CarSim math models are valid for full nonlinear 3D motions of rigid bodies. The components that have significant effect on handling, braking, and acceleration are represented with nonlinear tables of measurable data. The used vehicle model for the simulation is the F-class model with specifications summarized in Table 2. Simulations were conducted for two double lane change manoeuvres of 3 and 5 seconds. To demonstrate the robustness of the designed controllers, the simulation was done for low (0.3) and high (0.9) frictions and a longitudinal velocity of 30 m/s. Figures 4 and 5 illustrate the simulation results for the manoeuvre of 5 seconds. Figures 6 and 7 illustrate the simulation results for the manoeuvre of 3 seconds. Insets (a) depict the simulated and desired vehicle paths. Insets (b) depict the sliding surface of the proposed controller. Insets (c) and (d) illustrate the position and orientation errors with respect to time. Insets (e) and (h) show the steering of the vehicle (control output), the yaw angle, slip angle, and the roll angle of the vehicle, respectively.

For higher frictions and different manoeuvres, the performance of both controller are almost the same.

However, the performance of the proposed controller in eliminating the position error is remarkable. In terms of the steering angle, the proposed controller has lower effort, but associated with it some variations which should be addressed in the future works. For lower frictions, the performance of the proposed controller is evidently significant. For manoeuvre of 5 seconds, the controller shows better results, particularly in minimizing the position and orientation errors and achieving the full tracking. In terms of the roll angle, the proposed controller shows better results again. For manoeuvre of 3 seconds, the controller has preserved its good performance which results in low roll slip angles. The variations of the steering in this manoeuvre is significant, and their effect on the path is evident. As it is shown in Figure 7(a), the vehicle has some low-amplitude variations about its desired path, which are results of the variations in the performance of the controller. In all manoeuvres and under any condition, the sliding surface has approached towards zero and the vehicle has shown an acceptable stability. This indicates that our novel integrated controller has good performance.

6. CONCLUSION

In this paper, using a 5th degree polynomial function and dynamical constraints of vehicle, the double lane change path for two manoeuvre length of 3 and 5 seconds has been designed. A novel controller which utilized combination/integration of a backstepping and sliding mode controllers have been proposed. The stability of the proposed controller has been proved by defining a suitable Lyapunov function and proving its stability analysis. There are some constant parameters in the design of every controller which finding the optimum value of these parameters is a time demanding process. Therefore, the proposed controller's parameter has been optimized by using the PSO method. The defined cost function is a sum of absolute values of sliding surfaces and control effort. The simulation of this study has been conducted by linking the Simulink to CarSim Software which results in a non-linear full vehicle model with steering and suspension subsystems. This controller has been simulated for different frictions. The results of the simulation indicated proper tracking of the proposed controller compared to the backstepping controller.
The summary of this study achievement is as follows:

1. Stability analysis of an integrated sliding mode controller and backstepping controller has been proved analytically.
2. Integrated sliding mode controller and backstepping controller has better performance versus to sliding mode controller especially in the lower bound of uncertainty.
3. Adding a meta-heuristic optimization algorithm for finding the constant coefficients of the proposed controller is helpful to reduce tracking error.
4. Using meta-heuristic optimization increase the runtime of the system.

Taking into account the use of a meta-heuristic algorithm, reducing the running time of the proposed control law, and real-time tests for proposed controller will be introduced as future works.

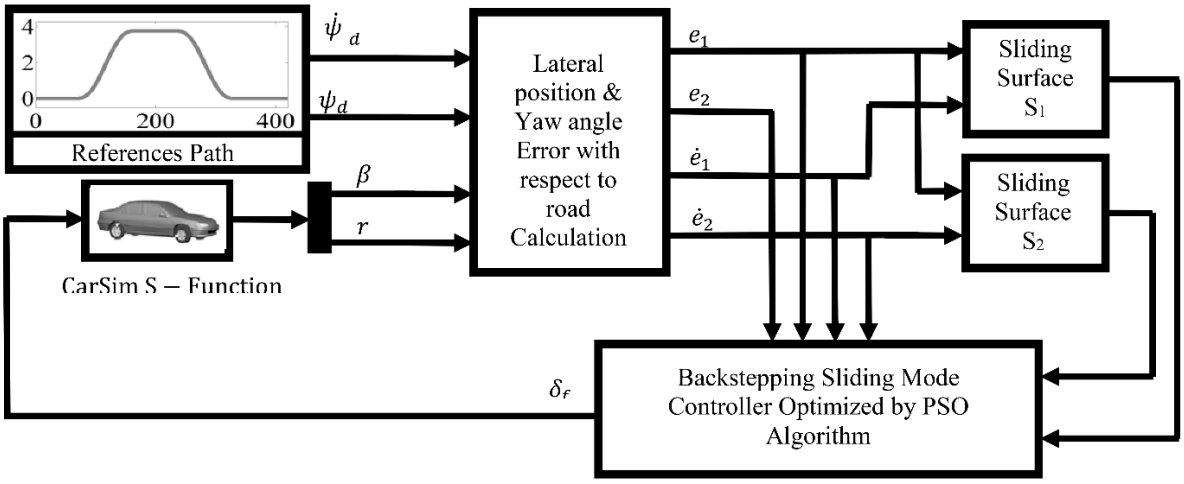

Figure3. The controlling diagram of the proposed integrated control

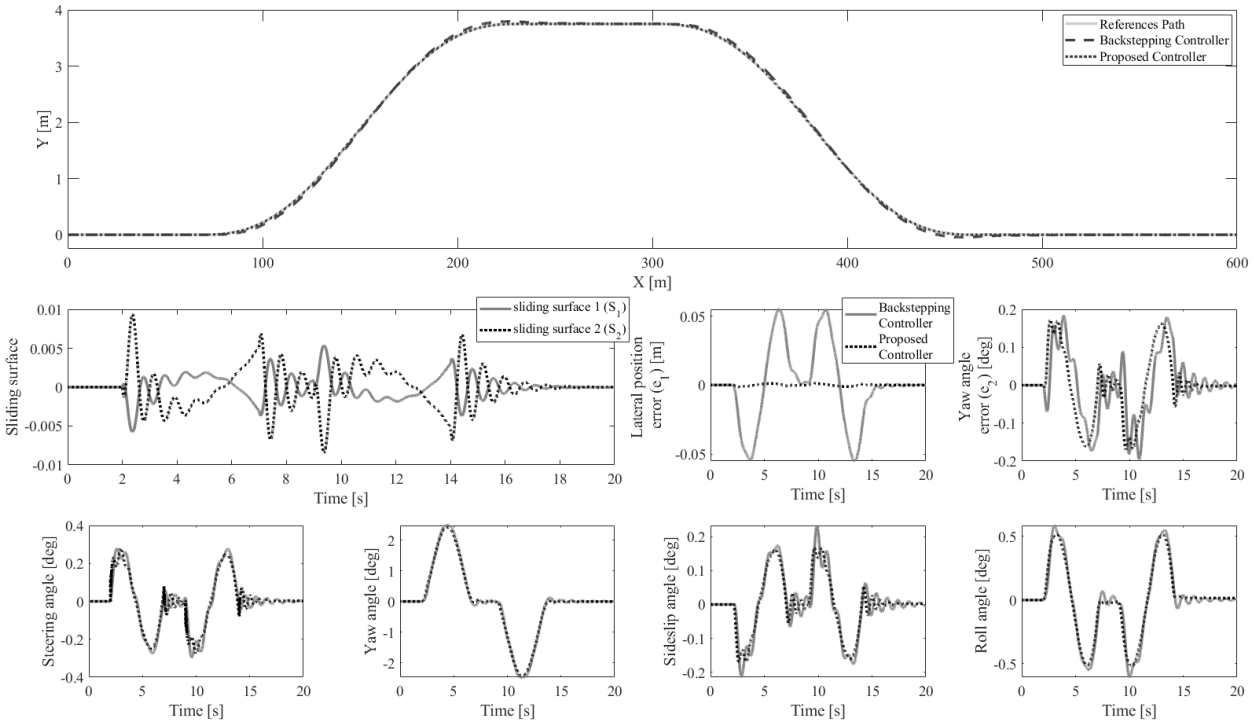

Figure 4. The simulation of backstepping controller and the proposed controller for manoeuvre of 5 seconds and friction of 0.9

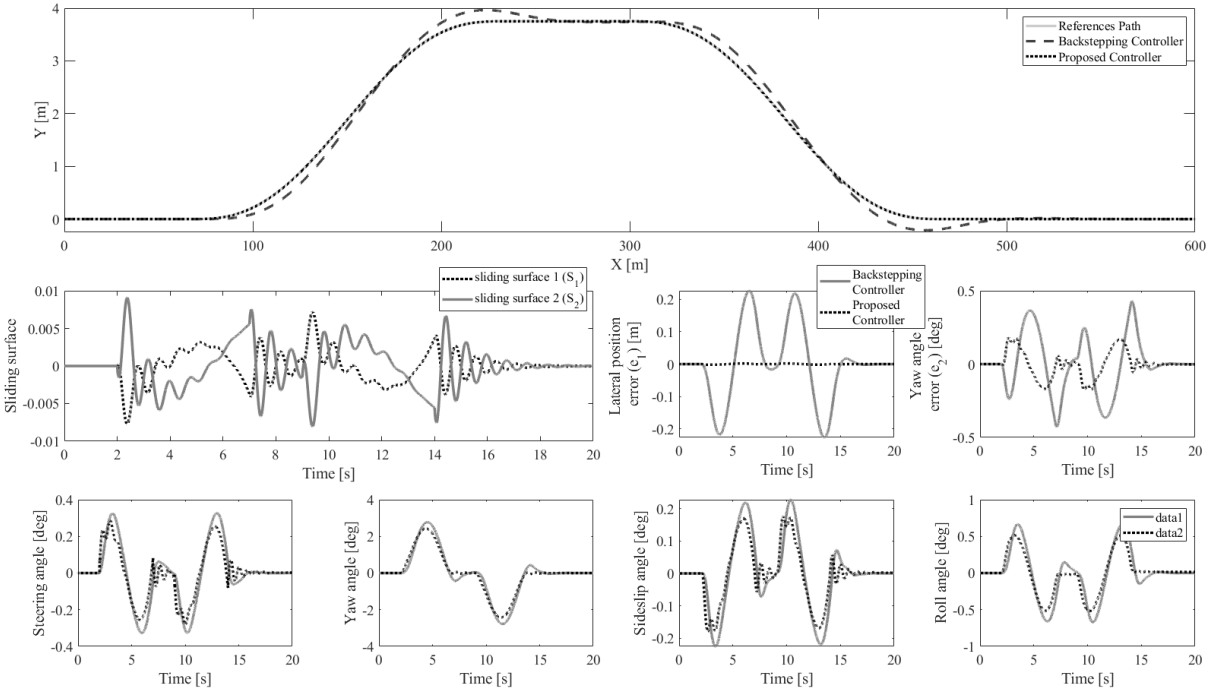

Figure 5. The simulation of backstepping controller and the proposed controller for manoeuvre of 5 seconds and friction of 0.3

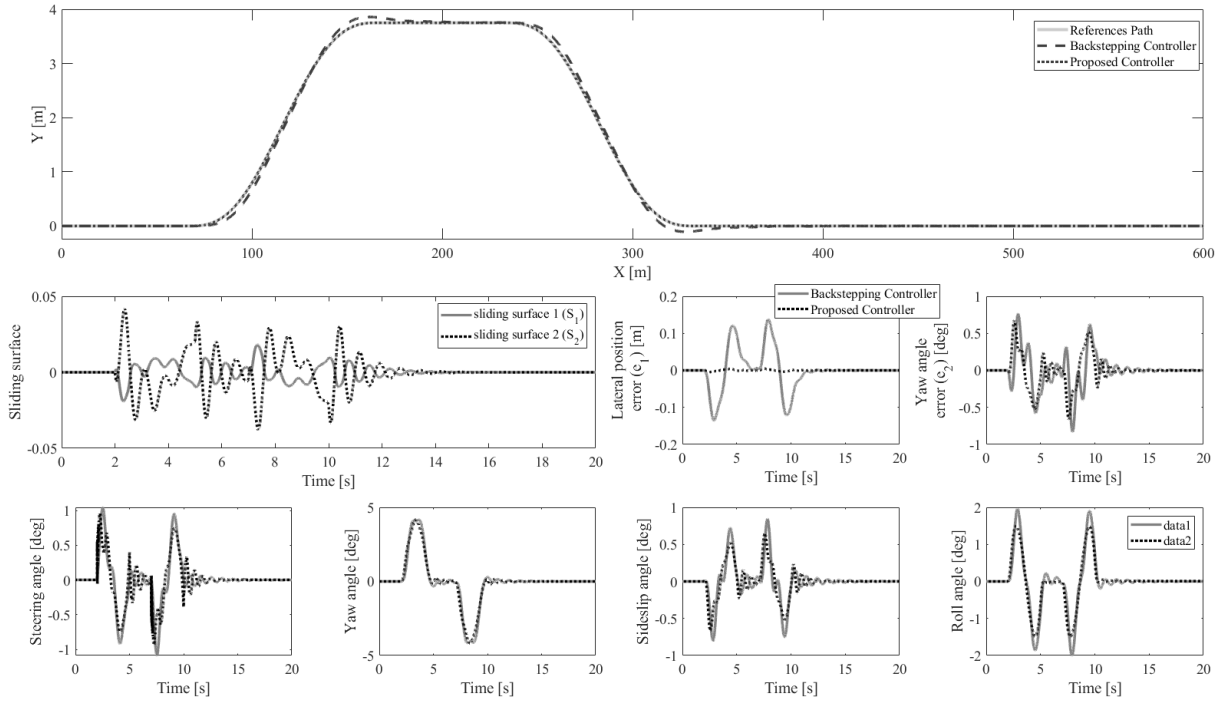

Figure 6. The simulation of backstepping controller and the proposed controller for manoeuvre of 3 seconds and friction of 0.9

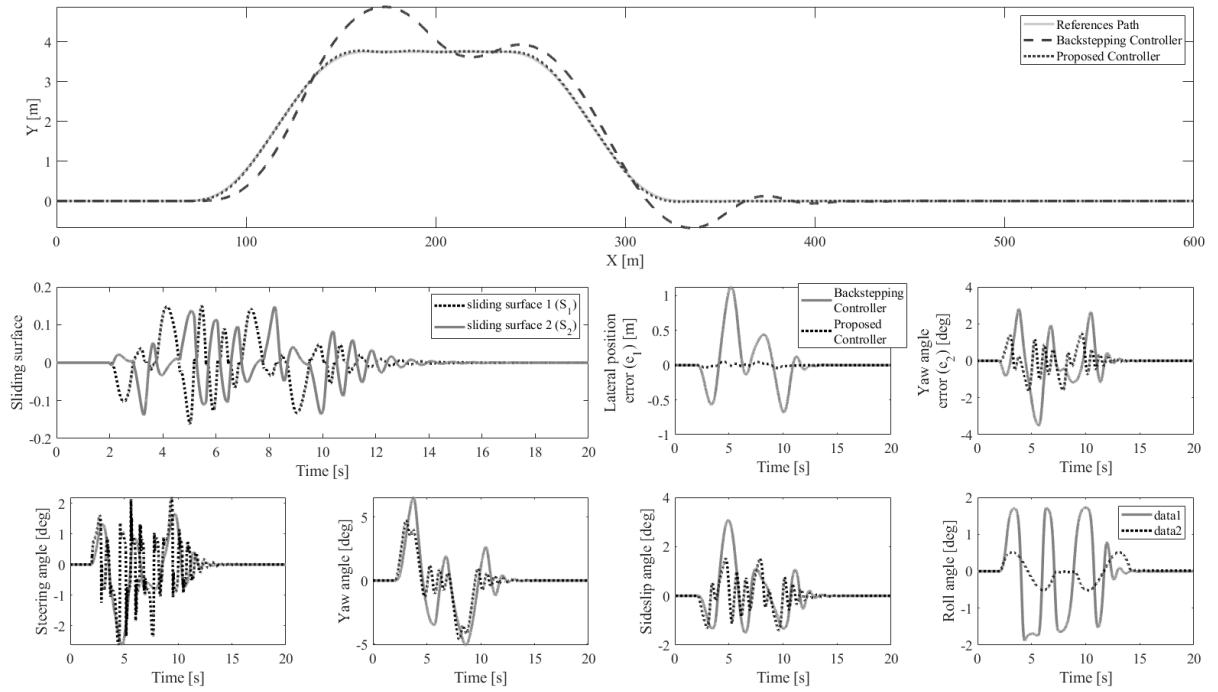

Figure7. The simulation of backstepping controller and the proposed controller for manoeuvre of 3 seconds and friction of 0.3

REFERENCES

1. Wierwille WW, Hanowski R, Hankey J, et al. *Identification and evaluation of driver errors: Overview and recommendations*. 2002.
2. Urmson C, Anhalt J, Bagnell D, et al. Autonomous driving in urban environments: Boss and the urban challenge. *Journal of Field Robotics* 2008; 25: 425-466.
3. Kemao P, Sam Y, Ismail M, et al. A Review on Integrated Active Steering and Braking Control for Vehicle Yaw Stability System. 2014.
4. Li B and Fu Z-J. Coordinated control of active steering and active roll control systems for enhanced vehicle lateral dynamics. *International Journal of Vehicle Performance* 2016; 2: 418-434.
5. Park J, Kim D, Yoon Y, et al. Obstacle avoidance of autonomous vehicles based on model predictive control. *Proceedings of the Institution of Mechanical Engineers, Part D: Journal of Automobile Engineering* 2009; 223: 1499-1516.
6. Abe M. Vehicle dynamics and control for improving handling and active safety: From four-wheel steering to direct yaw moment control. *Proceedings of the Institution of Mechanical Engineers, Part K: Journal of Multi-body Dynamics* 1999; 213: 87-101. DOI: 10.1243/1464419991544081.
7. Khalil HK. *Noninear Systems*. Prentice-Hall, New Jersey, 1996.
8. Guo L, Ge P-S, Yue M, et al. Lane changing trajectory planning and tracking controller design for intelligent vehicle running on curved road. *Mathematical Problems in Engineering* 2014; 2014.
9. Feng Y, Rongben W and Ronghui Z. Algorithm on lane changing and tracking control technology for Intelligent Vehicle. In: *Robotics and Biomimetics, 2007 ROBIO 2007 IEEE International Conference on* 2007, pp.1888-1893. IEEE.
10. Akar M and Kalkkuhl JC. Lateral dynamics emulation via a four-wheel steering vehicle. *Vehicle System Dynamics* 2008; 46: 803-829.
11. Hiraoka T, Nishihara O and Kumamoto H. Automatic path-tracking controller of a four-wheel steering vehicle. *Vehicle System Dynamics* 2009; 47: 1205-1227.
12. He J, Crolla DA, Levesley M, et al. Coordination of active steering, driveline, and braking for integrated vehicle dynamics control. *Proceedings of the Institution of Mechanical Engineers, Part D: Journal of Automobile Engineering* 2006; 220: 1401-1420.
13. Kunnappillil Madhusudhanan A, Corno M and Holweg E. Sliding mode-based lateral vehicle dynamics control using tyre force measurements. *Vehicle System Dynamics* 2015; 53: 1599-1619.
14. Lei J, Wu H, Yang J, et al. Sliding mode lane keeping control based on separation of translation and rotation movement. *Optik-International Journal for Light and Electron Optics* 2016; 127: 4369-4374.
15. Janbakhsh AA, Bayani Khaknejad M and Kazemi R. Simultaneous vehicle-handling and path-tracking improvement using adaptive dynamic surface control via a steer-by-wire system. *Proceedings of the Institution of Mechanical Engineers, Part D: Journal of automobile engineering* 2013; 227: 345-360.
16. Li L, Lian J, Wang M, et al. Fuzzy Sliding Mode Lateral Control of Intelligent Vehicle Based on Vision. *Advances in Mechanical Engineering* 2013; 5: 216862.
17. Guo J, Li L, Li K, et al. An adaptive fuzzy-sliding lateral control strategy of automated vehicles based on vision navigation. *Vehicle System Dynamics* 2013; 51: 1502-1517.
18. Alipour H, Bannae Sharifian MB and Sabahi M. A modified integral sliding mode control to lateral stabilisation of 4-wheel independent drive electric vehicles. *Vehicle System Dynamics* 2014; 52: 1584-1606.
19. Li L, Wang H, Lian J, et al. A lateral control method of intelligent vehicle based on fuzzy neural network. *Advances in Mechanical Engineering* 2014.
20. Feng J, Ruan J and Li Y. Study on intelligent vehicle lane change path planning and control simulation. In: *Information Acquisition, 2006 IEEE International Conference on* 2006, pp.683-688. IEEE.
21. Salehpour S, Pourasad Y and Taheri SH. Vehicle path tracking by integrated chassis control. *Journal of central south university* 2015; 22: 1378-1388.
22. Hegazy S, Rahnejat H and Hussain K. Multi-body dynamics in full-vehicle handling analysis. *Proceedings of the Institution of Mechanical Engineers, Part K: Journal of Multi-body Dynamics* 1999; 213: 19-31.
23. Norouzi A, Kazemi R and Azadi S. Vehicle lateral control in the presence of uncertainty for lane change maneuver using adaptive sliding mode control with fuzzy boundary layer. *Proceedings of the Institution of Mechanical Engineers, Part I: Journal of Systems and Control Engineering* 2018; 232: 12-28.
24. Rajamani R. *Vehicle dynamics and control*. Springer Science & Business Media, 2011.
25. Segel L. Theoretical prediction and experimental substantiation of the response of the automobile to steering control. *Proceedings of the Institution of Mechanical Engineers: Automobile Division* 1956; 10: 310-330.

Appendix 1

Table 2. The vehicle parameters in this study

Symbol	Description	Quantity
m	Mass	1704.7 [kg]
I_z	Yaw moment of inertia	3048.1 [kg.m^2]
l_f	Front axle-COG distance	1.035 [m]
l_r	Rear axle-COG distance	1.655 [m]
C_f	Cornering stiffness of front tire	105850 [N/rad]
C_r	Cornering stiffness of the rear tire	79030 [N/rad]
μ	Road friction coefficient	[0.3-0.9]
V_x	Longitude velocity	30 m/s
t_i	lane change manoeuvres start time	
t_f	lane change manoeuvres end time	
δ	Front wheel steering angle	
ψ_d	Desired yaw rate from road	
e_1	Lateral position error concerning the road	
e_2	Yaw angle error concerning the road	
λ	Thickness of the boundary layer	
K	Switching gain of proposed controller	
η	Constant Value in Lyapunov stability proof	
S	Sliding surface matrix	
V	Lyapunov function	
u_B	Controller output of backstepping controller	
$u_{B.S}$	Controller output of backstepping-sliding surface based on PSO optimization controller	

Appendix 2

Table 3.Abbreviated terms in this paper

Abbreviated term	Description
4WS	Four-wheel Steering
AFS	Active front steering
SBW	Steer by wire
DYC	Direct yaw moment control
ARS	Active rear steering
4WAS	Active front steering and four- wheel active steering